diversity

MDPI

Article

Integrated Genetic and Statolith Shape Analysis Reveals the Population Structure of *Loliolus* (*Nipponololigo*) *uyii* (Cephalopoda: Loliginidae) in the Coastal Waters of China

Xiaorong Wang [1,2], Chi Zhang [1] and Xiaodong Zheng [1,2,*]

[1] Key Laboratory of Mariculture, Ministry of Education, Ocean University of China, Qingdao 266003, China; xrwang@stu.ouc.edu.cn (X.W.); zhangchi6962@ouc.edu.cn (C.Z.)
[2] MOE Key Laboratory of Evolution & Marine Biodiversity and Institute of Evolution and Marine Biodiversity, Ocean University of China, Qingdao 266003, China
* Correspondence: xdzheng@ouc.edu.cn

Abstract: Understanding population structure is a priority for evaluating population dynamics of commercially fished cephalopods under fishing pressure and environmental changes. This study employed a multidisciplinary approach to clarify the population structure of *Loliolus* (*Nipponololigo*) *uyii*, a common squid in inshore fisheries. Sampling was conducted multiple times to cover the distribution range across the East China Sea and South China Sea. High haplotype diversity was revealed by three gene markers (*COI*, *16S* and *ODH*). Two geographical clades with significant genetic differentiation were divided through phylogenetic trees and haplotype networks. The boundary between the two clades is delineated by the Dongshan population in the southern East China Sea. Furthermore, the neutrality tests and mismatch analysis suggested that *L.* (*N.*) *uyii* populations may have undergone population expansion. Correspondingly, statolith differences in lateral dome and posterior indentation, along with high classification success, further supported the genetic division. The overall difference in statolith shape also efficiently identified seasonal groups in the Beibu Gulf lacking genetic differentiation. This result offers new insights into the influence of genetic and environmental factors on statolith shape. The integrated results provide a comprehensive understanding of the population structure of *L.* (*N.*) *uyii*, laying the foundation for resource development and the conservation of the species.

Keywords: population differentiation; statolith morphological; genetic diversity; mitochondrial DNA; nuclear DNA

check for updates

Citation: Wang, X.; Zhang, C.; Zheng, X. Integrated Genetic and Statolith Shape Analysis Reveals the Population Structure of *Loliolus* (*Nipponololigo*) *uyii* (Cephalopoda: Loliginidae) in the Coastal Waters of China. *Diversity* **2024**, *16*, 674. https://doi.org/10.3390/d16110674

Academic Editor: Bert W. Hoeksema

Received: 5 September 2024
Revised: 27 October 2024
Accepted: 28 October 2024
Published: 2 November 2024

Copyright: © 2024 by the authors. Licensee MDPI, Basel, Switzerland. This article is an open access article distributed under the terms and conditions of the Creative Commons Attribution (CC BY) license (https://creativecommons.org/licenses/by/4.0/).

1. Introduction

Cephalopods play a crucial role in the marine ecosystem and are also of significant economic value, representing one of the most promising fisheries resources [1]. They are characterized by rapid growth rates and short lifespans, which make them more resilient in the face of environmental changes [2,3]. The family Loliginidae is a key taxonomic group of cephalopods, comprising a large variety of tropical and temperate shallow-water squids [4]. The China seas, as an overexploited ecosystem, are experiencing high fishing and environmental pressures, resulting in a significant decrease in commercial fisheries resources and impacting on species and communities [5,6]. Limited dispersal capacity, geographical barriers and varying marine environments can lead to population variability and more complex population structures for species [7–9]. In cases where populations are subjected to varying levels of exploitation, it is essential to understand the population structure and dynamics to enhance and improve the management and exploitation of their resources [10]. *Loliolus* (*Nipponololigo*) *uyii* is an economic squid from the Loliginidae family *Loliolus* genus, which has a small body size and limited migratory ability and mainly inhabits the western Pacific Ocean to the eastern Indian Ocean and is

also found in the waters of China [11]. Recent studies on *L.* (*N.*) *uyii* have mainly centered on its morphological characteristics, life history and phylogeny [12,13]. However, genetic differences among different geographic populations of *L.* (*N.*) *uyii* and their population structures have not yet been reported.

To obtain deeper insights into population diversity and genetic structure, combining molecular markers with statolith data analysis offers a more comprehensive perspective [14,15]. Molecular genetic markers are versatile tools for researching the genetic diversity of marine organisms and uncovering phylogenetic relationships [15–18]. At present, mitochondrial DNA (mtDNA) and nuclear DNA (nuDNA) markers, two common molecular markers, play important roles in revealing the genetic structure and dynamics of a population [19]. Mitochondrial DNA markers are widely applied in population genetics studies of cephalopods [20–23]. Nuclear genes can provide more genetic information about organisms and are equally effective in detecting a population's genetic structure [24]. Muhammad et al. [25] described the basic population structure of *Octopus minor* in Chinese waters using two nuclear genes: *rhodopsin* and *octopine dehydrogenase* genes. In addition, statoliths, as hard body tissues, are valuable for determining population structure, because they have a stable shape and contain important biological and ecological information that can be used to distinguish individuals of the same squid species found in regions with differing environments and to identify the ecological lifestyle and population structure [26–28].

In our study, we used two mitochondrial genes, *cytochrome c oxidase I* (*COI*) and *16S rRNA* (*16S*), and one nuclear gene, *octopine dehydrogenase* (*ODH*), in combination with statolith data to analyze the population diversity and genetic differentiation of the *L.* (*N.*) *uyii* in different regions along the Chinese coast to gain a deeper understanding of the genetic differences and phylogenetic relationships, and to extend a scientific basis for the utilization and the sustainable development of *L.* (*N.*) *uyii*.

2. Materials and Methods

2.1. Sample Collection and Processing

L. (*N.*) *uyii* were collected from the coast of the China Seas during 2019–2023. The sampling areas contained the Northern East China Sea (NECS), Southern East China Sea (SECS), Northern South China Sea (NSCS) and Beibu Gulf (BBG) (Table 1; Figure 1). The samples were obtained from local fishermen and were stored in ice during their transport back to the laboratory. Mantle muscle tissue was taken from squid samples and preserved in 100% ethanol. These tissue samples were kept at –30 °C until DNA extraction was performed. For each squid, the dorsal mantle length (DML, mm) and body weight (BW, 0.1 g) were measured, and the stages of gonad development were assessed through visual observation [14,29]. Squid statoliths were extracted, cleaned with an ultrasonic cleaner and then dried. Thereafter, statoliths were stored in centrifuge tubes for subsequent analysis.

Table 1. Statolith and genetic samples data for *L.* (*N.*) *uyii* in the China Seas.

Sample	Region	Stations	Individual	Year	Month
Statolith samples	NECS	NB	177	2019	12
				2020	12
				2021	1
	SECS	ND	112	2020	2, 12
		DS	49	2023	6
	NSCS	MM	59	2023	11
	BBG	BH	178	2020	6, 7, 10, 11
				2021	3, 4
				2023	11

Table 1. *Cont.*

Sample	Region	Stations	Individual	Year	Month
Genetic samples	NECS	ZS	10	2020	12
		NB	11	2021	1
	SECS	ND	26	2021	1
		DS	33	2020	9
	NSCS	MM	59	2023	11
	BBG	BH	19	2023	11

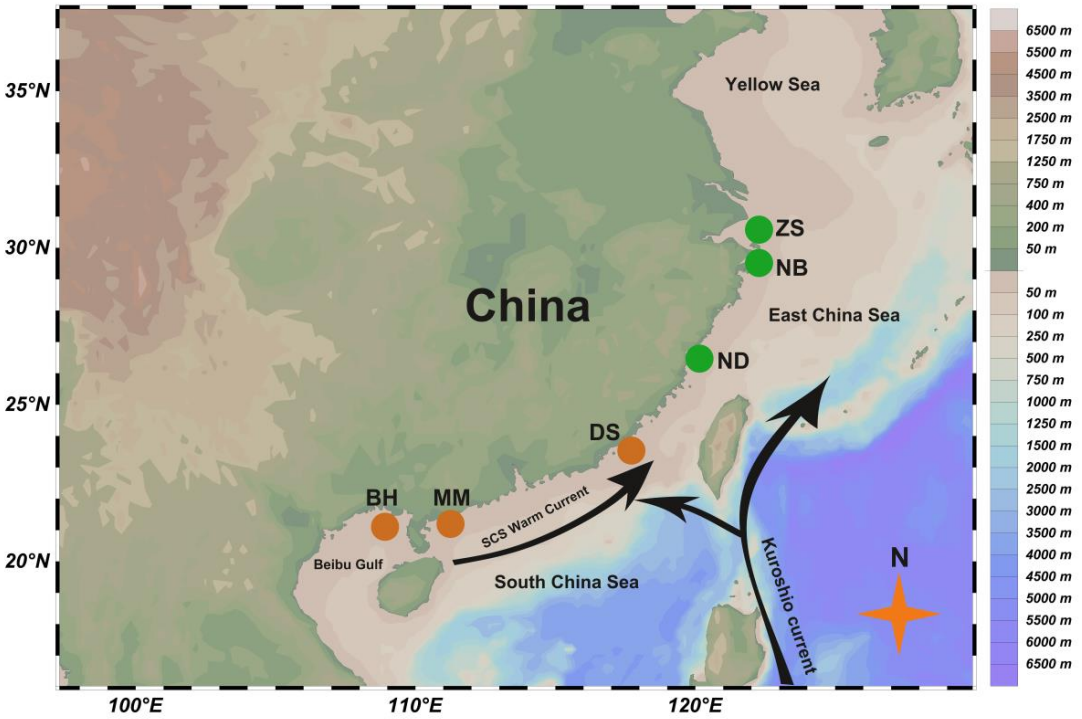

Figure 1. The sampling map for *L.* (*N.*) *uyii* from different locations. Zhoushan (ZS), Ningbo (NB), Ningde (ND), Dongshan (DS), Maoming (MM) and Beihai (BH). The green color represents the northern groups (ZS, NB and ND), and the orange color represents the southern groups (DS, MM and BH). The black arrows indicate ocean currents.

2.2. DNA Extraction and PCR Amplification

Total genomic DNA was extracted using the CTAB method modified by Winnepenninckx et al. [30]. The target genes were amplified by PCR using primers (Table 2). The amplification of target genes was reacted in a volume of 25 μL: 1 μL of 100 ng/μL DNA template, each primer 1 μL (10 μM/μL), 2 × Taq Master Mix 12.5 μL and 9.5 μL water. The PCR amplification cycle conditions were 95 °C for 3 min, 32 cycles of 95 °C for 15 s, 55 °C for 20 s, 72 °C for 1 min and a final extension step of 72 °C for 5 min. The products were detected by 1.5% agarose gel electrophoresis and sent to the Sangon Biotech Company (Shanghai, China) for sequencing.

Table 2. The primers of mitochondrial (mt) and nuclear (nu) genes.

Gene	Mt/Nu	Primers	Tm	Reference
COI	Mt	LCO1490: 5′-GGTCAAACAAATCATAAAGATATTGG-3′ HCO2198: 5′-TAAAATTCAGGGTGACCAAAAAATCA-3′	55	[31]
16S		16S-F: 5′-GCCTCGCCTGTTTACCAAAAAC-3′ 16S-R: 5′-CGGTCTGAACTCAGATCACGT-3′	55	[32]
ODH	Nu	ODH-F: 5′-ATGAGGGTTACTTTAGAGCCA-3′ ODH-R: 5′-GCAGGTCTTCATTGCCATAC-3′	55	Self-designed

2.3. Sequencing Analysis

2.3.1. Population Genetics

The SeqMan v.7.2 [33] in DNASTAR software package and MEGA v.11 [34] were used for sequence assembly and alignment. MEGA v.11 [34] was further utilized to compute the average base composition, the number of variable sites and genetic distances for all sequences. The DnaSP v 6.1 [35] software was employed to calculate genetic diversity indices and to infer population demographic history by constructing mismatch distribution plots for all populations and lineages of *L.* (*N.*) *uyii*. The haplotype network maps were constructed with Popart v.1.7 [36] and then manually adjusted. The genetic differentiation indices (F_{st}) can explore the level of genetic differentiation among populations. An Analysis of Molecular Variance (AMOVA) with the Kimura-2-parameters model, and neutrality tests, Tajima's *D* [37] and Fu's *Fs* tests [38], were determined with the Arlequin 3.5 [39].

2.3.2. Phylogenetic Relationship

Four datasets were constructed for phylogenetic analysis; the first three datasets consisted of haplotype sequences of *COI*, *16S* and *ODH* genes, respectively, and a concatenation of three genes from the same individual in the fourth dataset. The three genes were linked using the Phylosuite v 1.2.2 software [40], and the best nucleotide substitution models for each dataset were calculated using ModelFinder [41] under the BIC (Bayesian Information Criteria) criterion (Table S1). The ML (Maximum Likelihood) trees and BI (Bayesian Inference) trees based on four datasets were constructed by IQ-TREE v1.6.12 [42] and MrBayes v.3.2 [43], respectively. Finally, FigTree v1.4.4 (http://tree.bio.ed.ac.uk/software/figtree, accessed on 10 June 2024) was used to edit and visualize the ML and BI trees.

2.4. Statolith Shape Sampling and Statistical Analysis

To avoid the influence of individual development on statolith shape, only mature individuals (Stages III, IV and V) within an appropriate range of body length were chosen for subsequent morphological analysis of statoliths [14,29]. Previous studies have indicated the highly similar microstructural appearance of left and right statoliths, thus we randomly selected one statolith from each pair for photography and image analysis [44,45]. The statoliths were placed on a black background and photographed using a stereomicroscope (model: Nikon SMZ 18, Japan) equipped with a camera.

Using the "shapeR" package [46] for statolith image analysis, we extracted the contours of sample statoliths, visualized and generated shape data and transformed the contours into 45 normalized elliptical Fourier coefficients. This package was utilized to measure statolith length, width and area, and to calculate Sw/Sl (statolith width/length) and standard statolith area (Ssa = 1000 × (statolith area/DML^2)). Discriminant analysis of species was conducted using the Random forest (RF) package [47] version 4.7 in R, with the out-of-bag (OOB) evaluation assessing the accuracy of the random forest algorithm. Data visualization was performed by the Multidimensional Scaling (MDS) model based on the RF package to assess the similarities and differences among statolith data from different areas.

3. Results

3.1. Genetic Analysis

3.1.1. Gene Sequences and Population Diversity

In this study, 136 partial *COI* sequences, 137 partial *16S* sequences and 113 *ODH* partial sequences of *L.* (*N.*) *uyii* were obtained. The sequence characteristics are shown in Table 3. There were some differences in the base composition of each gene, but the average percentage of T was the highest for each gene, and the content of A + T was higher than that of G + C, with an apparent AT composition bias. The *COI* sequences exhibited the highest proportion of variable sites and the highest degree of variation (9.4%), while the *ODH* gene showed the lowest degree of variation (3.2%). The mitochondrial gene sequences showed higher levels of variation compared to the nuclear gene.

Table 3. Molecular characterization based on mitochondrial and nuclear gene sequences.

Mt/Nu	Gene	Length/bp	T/%	C/%	A/%	G/%	A + T/%	G + C/%	V	Pi	S	Proportion of Variable Sites/%
Mt	*COI*	616	35.7	20.2	28.8	15.3	64.5	35.5	58	48	10	9.4
	16S	478	39.8	9.3	33.3	17.7	73.1	27.0	21	12	9	4.4
Nu	*ODH*	537	28.0	23.3	24.8	23.9	52.8	47.2	17	9	8	3.2

A total of 18 *COI* haplotypes, 13 *16S* haplotypes and 19 *ODH* haplotypes were defined for the *L.* (*N.*) *uyii* populations from different seas. Based on the *COI* and *16S* genes, the haplotype diversity and nucleotide diversity of all individuals were generally high (*COI*: 0.559 and 0.0341; *16S*: 0.508 and 0.0101), whereas the *ODH* sequences displayed high haplotype diversity but low nucleotide diversity. The analysis of the three genes consistently revealed that the NECS and BBG populations had lower nucleotide diversity, while the SECS populations had higher haplotype diversity. The Northern South China Sea (NSCS) population displayed relatively lower diversity because the Hd and π values were low (Table 4).

Table 4. The genetic diversity indices for populations of *L.* (*N.*) *uyii*.

Group	*COI*				*16S*				*ODH*			
	N	Hap	Hd	π	N	Hap	Hd	π	N	Hap	Hd	π
NECS	21	6	0.552	0.0010	17	3	0.228	0.0005	21	3	0.338	0.0008
SECS	53	11	0.665	0.0385	55	6	0.571	0.0118	49	10	0.740	0.0044
NSCS	43	2	0.047	0.0002	46	6	0.208	0.0008	27	6	0.399	0.0012
BBG	19	3	0.205	0.0003	19	1	0.000	0.0000	16	7	0.692	0.0018
Total	136	18	0.559	0.0341	137	13	0.508	0.0101	113	19	0.722	0.0044

3.1.2. Haplotype Distribution and Phylogenetic Relationships

The 18 haplotypes of *COI* sequences, containing 3 shared haplotypes and 15 unique haplotypes, were differentiated into a two star-structure centered on Hap1 and Hap8, respectively, with deletion haplotypes occurring between the two groups (Figure 2). The *16S* gene had the fewest haplotypes, with Hap1 and Hap4 being shared and appearing most frequently (Figure 3). There were five shared haplotypes in *ODH* gene haplotypes, including Hap1, Hap3, Hap6, Hap8, Hap10, with a higher distribution of haplotypes and the presence of deletion haplotypes in Clade B (Figure 4). Compared to mitochondrial genes, nuclear genes showed fewer mutational steps between the two lineages.

The phylogenetic trees of the haplotype sequences were structured by Maximum Likelihood (ML) and Bayesian Inference (BI) methods, and the phylogenetic results of three genes were in accordance with the haplotype network. Both the trees and haplotype networks of the three genes informed two distinct branches (Figures 2–4), and all displayed that the haplotypes of the three geographic groups located in the Northern East China Sea (ZS and NB) and the Southern East China Sea (ND) were clustered together in Clade A, and the Clade B included haplotypes from the DS (the Southern East China Sea), MM (the Northern South China Sea) and BH (the Beibu Gulf). The results of the combined phylogenetic analysis of multiple genes based on the ML and BI methods were in agreement with the single-gene results, and the *L.* (*N.*) *uyii* populations were classified into two groups same as single-gene (Figure 5).

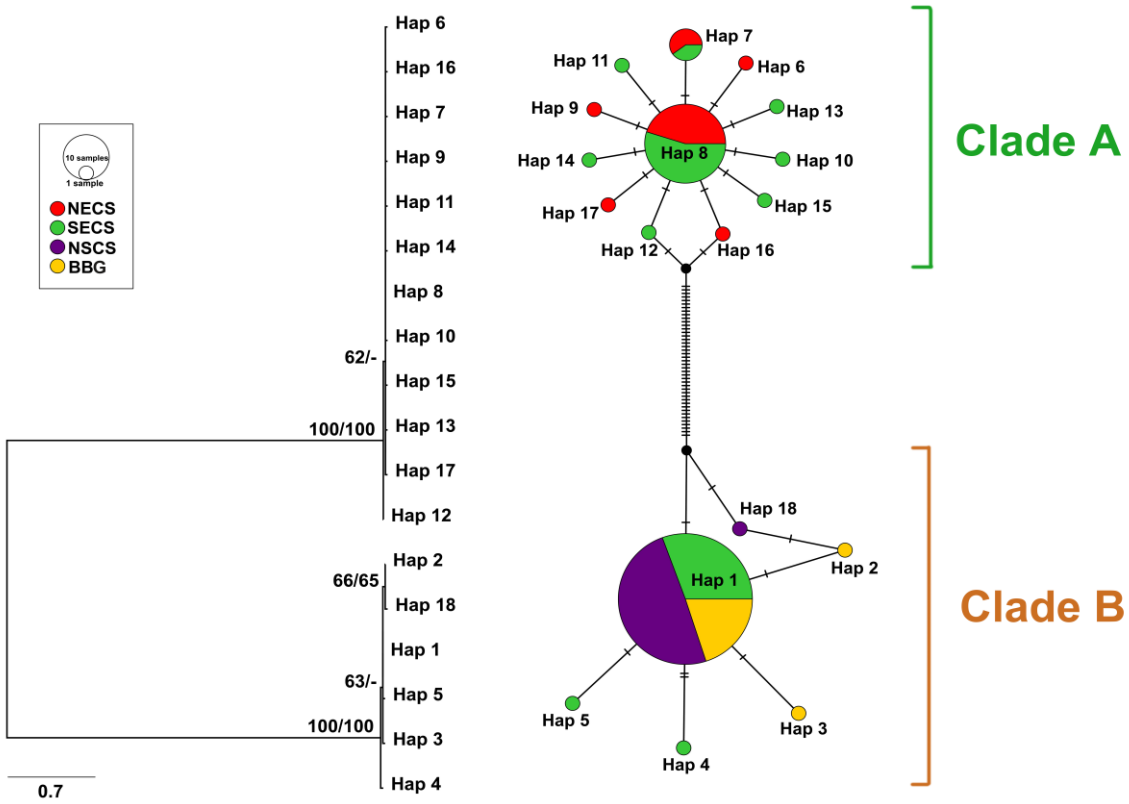

Figure 2. Maximum likelihood (ML) and Bayesian inference (BI) phylogenetic tree and haplotype network of *L.* (*N.*) *uyii* based on *COI* haplotypes. Branch numbers are bootstraps (**left**) and posterior probability (**right**). Black dots represent hypothetical missing intermediates.

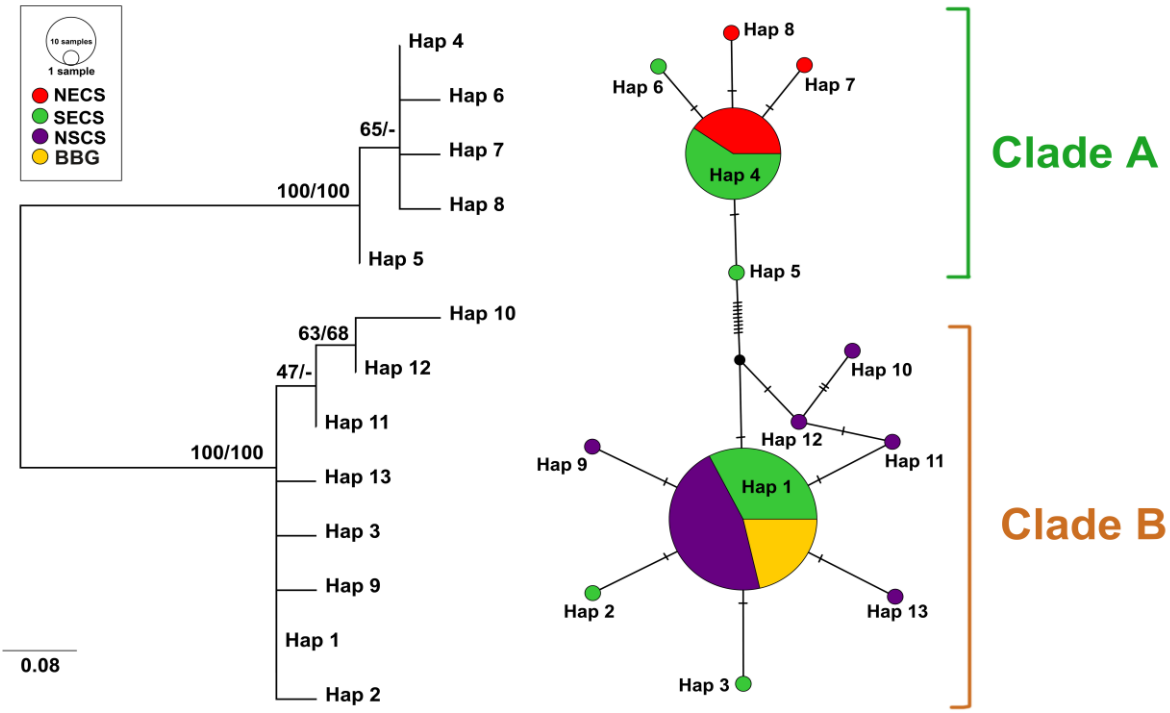

Figure 3. Maximum likelihood (ML) and Bayesian inference (BI) phylogenetic tree and haplotype network of *L.* (*N.*) *uyii* based on *16S* haplotypes. Branch numbers are bootstraps (**left**) and posterior probability (**right**). Black dots represent hypothetical missing intermediates.

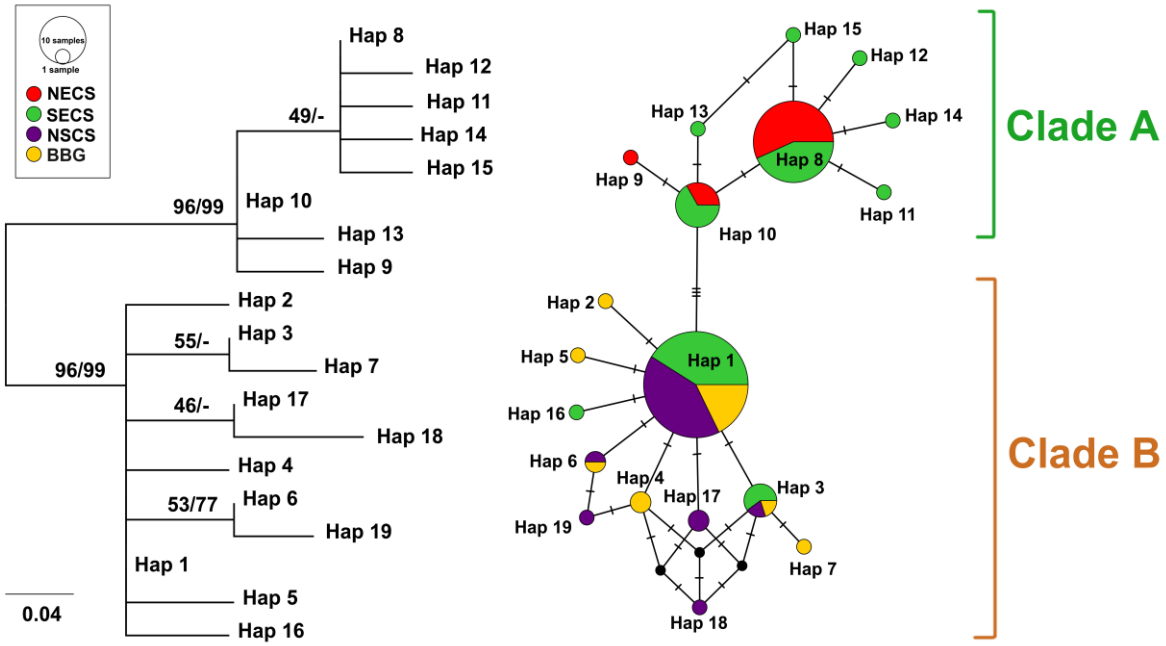

Figure 4. Maximum likelihood (ML) and Bayesian inference (BI) phylogenetic tree and haplotype network of *L.* (*N.*) *uyii* based on *ODH* haplotypes. Branch numbers are bootstraps (**left**) and posterior probability (**right**). Black dots represent hypothetical missing intermediates.

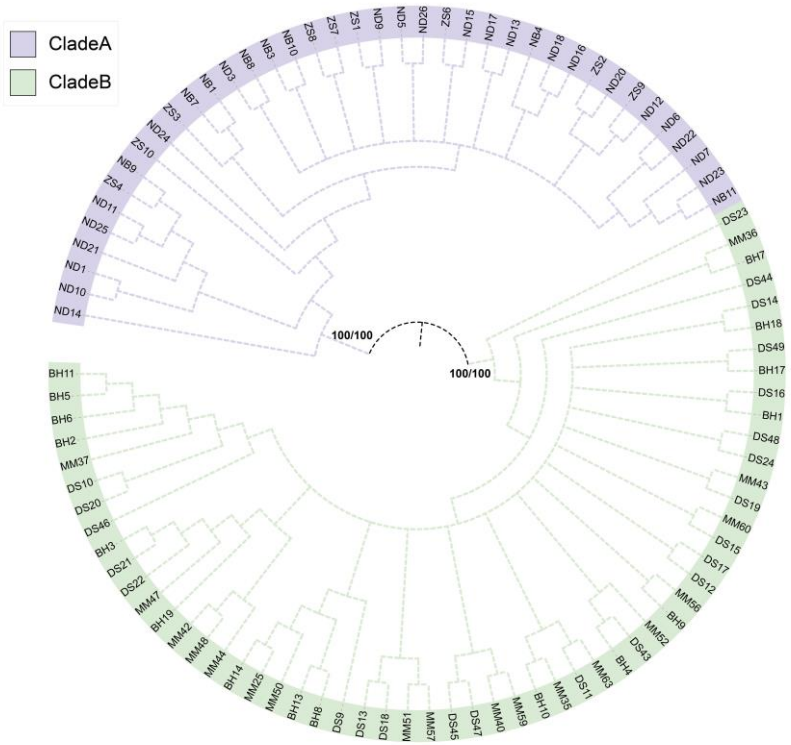

Figure 5. Phylogenetic trees constructed using the concatenation of mitochondrial and nuclear genes. The numbers in each node represent bootstraps of maximum likelihood (ML) and posterior probabilities of Bayesian inference (BI) analyses, respectively. The purple color represents the Clade A and the green color represents the Clade B.

3.1.3. Population Structure and Demographic History

The possible genetic variation between Clade A (ZS, NB and ND) and Clade B (DS, MM and BH) was investigated using AMOVA and F_{st} analyses. The results of AMOVA analysis based on the three genes were consistent, revealing that the genetic difference in the *L.* (*N.*) *uyii* populations was dominated by the variation among the two groups, and the percentage of variation was higher in mitochondrial genes than in nuclear genes (Table 5). The F_{st} analyses of all the genes indicated that there was no genetic differentiation between the NSCS (MM) and BBG (BH) populations ($F_{st} < 0$), but high and significant F_{st} values were found between these two populations and the NECS (ZS and NB) population. The F_{st} values between the SECS population (ND and DS) and the other populations were greater than 0.25 and were significant (Tables 6 and 7). Between Clade A and Clade B, the F_{st} values were 0.993 (*COI*), 0.980 (*16S*) and 0.855 (*ODH*), respectively ($p < 0.05$) (Table S2). Subsequently, genetic distances were calculated between and within the two lineages based on the three genes (Table S2), and the genetic distance between the lineages of *COI* sequences was 5.65%, which was the most significant among the three genes. The results demonstrated significant genetic differences between the two lineages of the *L.* (*N.*) *uyii* populations, supporting the haplotype and phylogenetic results.

Table 5. AMOVA analysis of *L.* (*N.*) *uyii* populations based on mitochondrial and nuclear gene sequences.

Gene	Source of Variation	df	Variance Component	Percentage of Variation (%)	*F* Statistic
COI			Gene pool (Clade A; Clade B)		
	Among groups	1	22.93516 Va	99.32	FSC: 0.001 ($p = 0.000$)
	Among populations within groups	4	0.00015 Vb	0.00	FST: 0.993 ($p = 0.753$)
	Within populations	130	0.15766 Vc	0.68	FCT: 0.993 ($p = 0.092$)
	Total	135	23.09297		
16S			Gene pool (Clade A; Clade B)		
	Among groups	1	5.45493 Va	98.04	FSC: 0.004 ($p = 0.000$)
	Among populations within groups	4	0.00045 Vb	0.01	FST: 0.980 ($p = 0.294$)
	Within populations	131	0.10865 Vc	1.95	FCT: 0.980 ($p = 0.103$)
	Total	136	5.56402		
ODH			Gene pool (Clade A; Clade B)		
	Among groups	1	1.79249 Va	85.51	FSC: –0.012 ($p = 0.000$)
	Among populations within groups	4	–0.00363 Vb	–0.17	FST: 0.853 ($p = 0.679$)
	Within populations	107	0.30733 Vc	14.66	FCT: 0.855 ($p = 0.117$)
	Total	112	2.09619		

Table 6. F_{st} between populations of *L.* (*N.*) *uyii* based on *COI* (below diagonal) and *16S* (above diagonal).

Group	NECS	SECS	NSCS	BBG
NECS		0.4334 *	0.9694 *	0.9900 *
SECS	0.4148 *		0.3802 *	0.3144 *
NSCS	0.9942 *	0.4300 *		–0.0079
BBG	0.9906 *	0.3520 *	–0.0054	

* Significant at $p < 0.05$.

Table 7. F_{st} between populations of *L.* (*N.*) *uyii* based on *ODH* gene.

Group	NECS	SECS	NSCS	BBG
NECS				
SECS	0.3458 *			
NSCS	0.8716 *	0.3183 *		
BBG	0.8488 *	0.2820 *	–0.0110	

* Significant at $p < 0.05$.

Based on the *COI* and *16S* sequences for Clade A and Clade B, the presence of negatives and the significant deviation from the neutral value in both Tajima′s *D* and Fu′s *Fs* tests suggested a departure from neutral evolutionary processes and that a population expansion event had occurred in the past (Table 8). The *ODH* gene analysis results of the two clades can also be used as evidence of a population expansion, showing that the Tajima′s *D* value of the Clade A was negative but not significant, and the other values were negative and significant (Table 8). The bimodal mismatch distributions were observed in total sequences based on three genes of *L.* (*N.*) *uyii*, which corresponded to the genetic differentiation of Clade A and Clade B (Figure S1). The unimodal mismatch distributions were detected in the two clades, further indicating a sustained population expansion happened in the two clades.

Table 8. Results of neutrality test for clades of *L.* (*N.*) *uyii* based on mitochondrial and nuclear gene sequences.

Group	*COI*		*16S*		*ODH*	
	Tajima's *D*	**Fu's *Fs***	**Tajima's *D***	**Fu's *Fs***	**Tajima's *D***	**Fu's *Fs***
Clade A	–2.2085 *	–12.4763 *	–1.8781 *	–5.0930 *	–1.3837	–5.2013 *
Clade B	–1.9864 *	–7.2394 *	–2.0846 *	–9.5896 *	–1.6717 *	–9.7917 *

* Significant at $p < 0.05$.

3.2. Statolith Morphological Analysis

3.2.1. Statolith Analyses Among Different Seas

Based on the Random Forest model constructed using Ssa, Sw/Sl and 45 Fourier coefficients, the BBG population achieved the highest recognition success rate of 86%, followed by NECS with 75%. In contrast, NSCS had the lowest recognition success rate at 25% (Table 9). The MDS plot illustrated relationships of statolith morphology across various area groups (Figure 6), notably highlighting clearer differentiation between the BBG and NECS, which was a more intuitive reflection of the Out-of-Bag (OOB) results. The reconstructed statolith average outlines from different areas indicated variations in statolith shape among the respective groups (Figure 7), which demonstrated distinctions between the northern and southern groups, particularly focused on the lateral dome and posterior indentation. The northern groups (NECS and SECS) had a raised lateral dome and relatively shallow posterior indentation. The southern groups (NSCS and BBG) had a slightly pointed dorsal dome.

Table 9. Out-of-Bag (OOB) estimation matrix of the random forest among the four regions.

Region	NECS	SECS	NSCS	BBG	Classification Success Rate (%)
NECS	133	35	0	9	75
SECS	63	73	1	24	45
NSCS	5	2	15	37	25
BBG	11	10	4	153	86

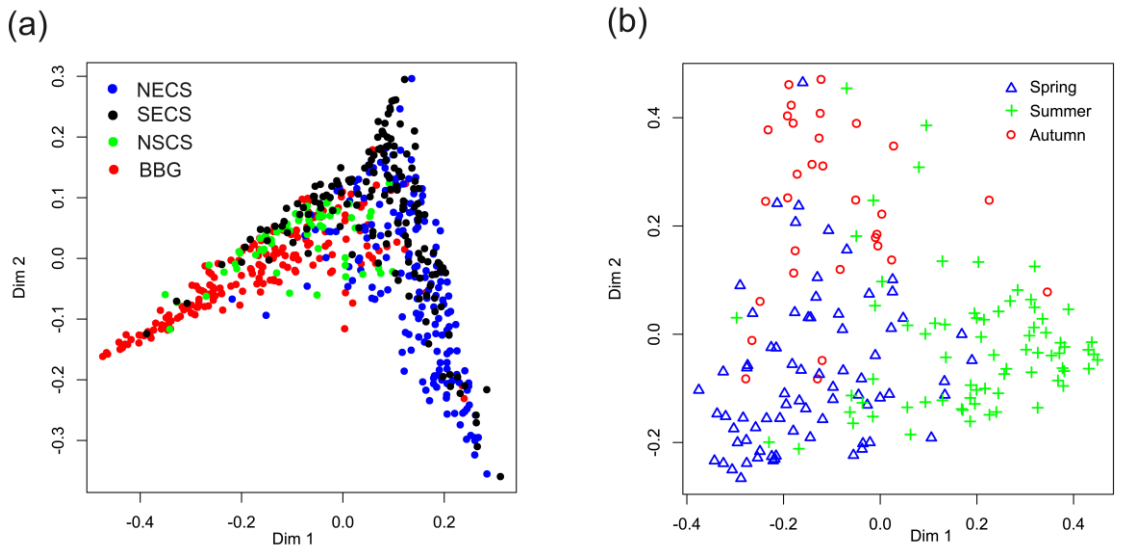

Figure 6. MDS plot of statolith morphology for different regions (**a**) and different seasons in BBG (**b**).

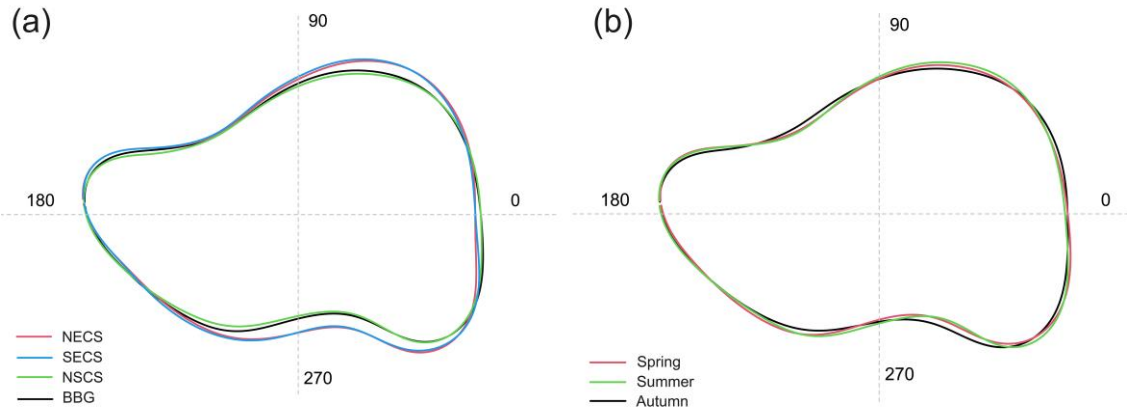

Figure 7. Reconstructed statolith outlines for different regions (**a**) and different seasons in BBG (**b**).

3.2.2. Statolith Analyses Among Different Seasons in the Beibu Gulf

The Out-of-Bag (OOB) estimation matrix of the random forest among three seasons revealed that the highest discrimination success rate exceeded 80% in both spring and summer (Table 10). The MDS plot depicted the relationships among the three distinct branches in different seasons (Figure 6). Additionally, the average statolith outlines revealed slight differences in the lateral dome and posterior indentation regions between spring and summer/autumn (Figure 7). The statolith difference appeared in overall outlines.

Table 10. Out-of-Bag (OOB) estimation matrix of the random forest among the three seasons in BBG.

Season	Spring	Summer	Autumn	Classification Success Rate (%)
Spring	63	8	3	85
Summer	9	61	3	84
Autumn	9	5	17	55

4. Discussion

4.1. Population Genetic Diversity of L. (N.) uyii

Genetic diversity is a key indicator for species resource development, utilization and conservation, reflecting the adaptive capacity and survival potential of species in the face of environmental change. Moreover, a high level of genetic diversity also enables species

to better cope with fluctuating environments [48–50]. Haplotype diversity and nucleotide diversity indices are important parameters for measuring genetic diversity in population genetics research [51]. In the present study, all populations of *L.* (*N.*) *uyii* showed high levels of haplotype diversity and nucleotide diversity in *COI* and *16S* gene sequences (Hd > 0.5, $\pi > 0.005$), reflecting a high level of mitochondrial gene diversity. However, the nuclear gene *ODH* exhibited high haplotype diversity and low nucleotide diversity (Hd > 0.5, $\pi < 0.005$), which could be due to rapid population growth and the accumulation of genetic mutations after a bottleneck effect [52]. Previous studies have demonstrated varying evolutionary rates among genes [53]. The nucleotide diversity of *COI* and *16S* genes was significantly higher than that of the *ODH* gene, indicating that mitochondrial genes evolve at a faster rate than the nuclear gene and the genetic diversity of *COI* and *16S* is greater than that of *ODH*. The observed difference in genetic diversity between mitochondrial and nuclear markers may be due to the maternal inheritance of mitochondrial genes [54]. Moreover, nuclear genes typically exhibit lower within-species variation [54], and genetic exchange among populations can further reduce sequence diversity in nuclear genes. Consequently, different resolutions may arise when using mitochondrial and nuclear gene markers for studies on genetic variation among populations. We employed two mitochondrial genes in combination with one nuclear gene to analyze genetic variation among populations, which can provide a more accurate assessment of genetic diversity and differentiation.

4.2. Genetic Structure and Historical Dynamics

Based on the phylogenetic tree and haplotype network analysis from three genes, *L.* (*N.*) *uyii* populations along the Chinese coast were divided into two major divergent branches. The differentiation between northern and southern lineages is delineated by the DS population in the southern East China Sea, with significant genetic divergence between the two lineages ($F_{st} > 0.25$, $p < 0.05$). Besides, the AMOVA results indicated that genetic differentiation primarily arises from variance between lineages. It should be noted that the neutrality test results indicated that the molecular markers in this study were non-neutral markers, and the F_{st} analysis of gene flow during the evolutionary process will be influenced by environmental factors [55]. Therefore, in subsequent research, it will be necessary to use SNPs and microsatellites to analyze neutral molecular markers. Many factors impact population structure and genetic differentiation, such as environmental tolerance, ocean currents and geographic barriers [8,56,57]. The Kuroshio current, a major boundary current of the Northwest Pacific, flows through the Luzon Strait and intrudes into the northeastern part of the South China Sea [58]. The South China Sea's warm current extends along the coastal shelf of Guangdong in southern China and flows into the Taiwan Strait [59]. These circulation patterns in the northern South China Sea may facilitate genetic exchange between the DS and South China Sea populations [60], which is why the DS, MM and BH localities form a clade in the phylogenetic trees. In addition, the higher temperature in the southern China Sea means that the differences in temperature between the southern and northern seas may also be an important factor in the differentiation of populations along the Chinese coast [23,61]. The higher temperature may cause higher metabolic and growth rates and a faster frequency of gene mutations, which may lead to genetic differences between two clades of *L.* (*N.*) *uyii* [5,53]. As with many ectothermic animals, temperature strongly influences cephalopod reproduction [62,63]. Because the optimal temperature range for reproduction is reached at different times (probably at different months) between southern and northern regions, *L.* (*N.*) *uyii* could only reproduce with individuals from the same oceanographic area [64]. This also could cause reproductive isolation and genetic variation between *L.* (*N.*) *uyii* from two regions. There are complex and variable water masses in the Chinese offshore, and physical barriers between water masses may hinder population dispersal and lead to genetic differentiation [61]. The analysis of the mismatch distribution and neutrality test results revealed that there has been a population expansion event in the evolutionary history of the *L.* (*N.*) *uyii* populations.

Species evolution and distribution are often influenced by historical geological events, such as tectonic changes, and climate fluctuations, including ancient geological events and climate change. These factors can impact genetic variation and are reflected in their genetic structure [65]. Two haplotype lineages were detected in the population of *L.* (*N.*) *uyii*, which are associated with different geographical regions. It is speculated that this could be due to geographical isolation caused by the sea level drop that occurred during the Pleistocene epoch in the western Pacific margin, and as the glaciers melted and sea levels rose, expansion events occurred, leading to secondary contact between the populations of the two lineages [22,66]. Accumulated genetic variations over time have resulted in significant genetic structures and potentially the presence of cryptic species, and the effect of Pleistocene climate oscillations on population structure has been extensively reported in different marine organisms [23,67,68].

4.3. Statolith Morphological Differentiation

The shape of cephalopod statoliths, like fish otoliths, may be regulated by both genetic and environmental factors [27,69]. Therefore, the statolith shape also can effectively identify populations, especially those living in variable environmental conditions [70]. In our study, analysis of statolith profiles from different geographical populations of *L.* (*N.*) *uyii* revealed higher classification success rates for the populations in the Beibu Gulf and northern East China Sea. Although a low classification rate was detected in SECS and NSCS, the majority misclassification was categorized to the adjacent population—namely NECS and BBG, respectively. Therefore, the analysis of statolith shape from different areas categorized the southern (BBG and NSCS) and northern (NECS and SECS) regions into two distinct groups, in agreement with the phylogenetic relationships revealed by genetic markers. The main shape difference was found in the lateral dome and posterior indentation, which is similar to the variation among five Loliginidae squid species [71]. Furthermore, statolith shape is highly sensitive to local conditions and can identify ecologically separated groups [14]. As expected, high classification success was also obtained in the Beibu Gulf among seasonal groups, while the statolith difference appeared in overall outlines, unlike the clear local difference between the two spatial populations. At present, many factors affecting statolith shape have not been fully identified, so the interpretation of analysis results will become complex [72]. The current result provides insight into the influence of genetic and environmental factors on statolith shape, as in fish otoliths, upon environment-induced overall outline change and genetically locally induced changes in prominent parts [73]. An improved knowledge of the factors that influence statolith shape could improve its use in population studies.

5. Conclusions

This study revealed the population structure of *L.* (*N.*) *uyii* using mitochondrial genes (*COI* and *16S*) and nuclear gene (*ODH*) sequences. Analysis of the three genes indicated significant genetic differentiation between the southern and northern marine regions of China. Additionally, the study of statolith shape in *L.* (*N.*) *uyii* populations was consistent with the genetic findings, showing differences in statolith shape between the southern and northern regions. These two methods provide a comprehensive understanding of the population structure of *L.* (*N.*) *uyii*, offering important genetic and developmental information for subsequent cephalopod research, extending a theoretical basis for the reasonable development and utilization of *L.* (*N.*) *uyii* fishery resources.

Supplementary Materials: The following supporting information can be downloaded at: https://www.mdpi.com/article/10.3390/d16110674/s1, Table S1: The best nucleotide substitution model based on gene sequences; Table S2: Mean genetic distances within (diagonal) and between (below diagonal) clades and *F*st (above diagonal) of *L. (N.) uyii* based on mitochondrial and nuclear gene sequences. Figure S1. Mismatch distribution based on mitochondrial and nuclear genes of *L. (N.) uyii*.

Author Contributions: X.Z., C.Z. and X.W. designed the study; X.W. performed the experiments and wrote the original draft; C.Z. collected the samples; X.Z. and C.Z. reviewed paper; All authors have read and agreed to the published version of the manuscript.

Funding: This work was supported by the National Natural Science Foundation of China (NO. 32170536).

Institutional Review Board Statement: All experiments were approved by the Institutional Animal Care and Use Committee of Ocean University of China.

Informed Consent Statement: Not applicable.

Data Availability Statement: Original gene sequences uploaded to GenBank (*COI*: PQ201376-PQ201511; *16S*: PQ198240-PQ198376; *ODH*: PQ208200-PQ208312).

Acknowledgments: The authors thank Shuiyou Lin and Nianping Cai for their assistance in sample collection.

Conflicts of Interest: The authors declare no conflicts of interest.

References

1. Arkhipkin, A.; Hendrickson, L.C.; Paya, I.; Pierce, G.J.; Roa-Ureta, R.H.; Robin, J.; Winter, A. Stock assessment and management of cephalopods: Advances and challenges for short-lived fishery resources. *ICES J. Mar. Sci.* **2021**, *78*, 714–730. [CrossRef]
2. Doubleday, Z.A.; Prowse, T.A.A.; Arkhipkin, A.; Pierce, G.J.; Semmens, J.; Steer, M.; Leporati, S.C.; Lourenco, S.; Quetglas, A.; Sauer, W.; et al. Global proliferation of cephalopods. *Curr. Biol.* **2016**, *26*, R406–R407. [CrossRef] [PubMed]
3. Rodhouse, P.G.K.; Pierce, G.J.; Nichols, O.C.; Sauer, W.H.; Arkhipkin, A.I.; Laptikhovsky, V.V.; Lipinski, M.R.; Ramos, J.E.; Gras, M.; Kidokoro, H.; et al. Environmental effects on cephalopod population dynamics: Implications for management of fisheries. *Adv. Mar. Biol.* **2014**, *67*, 99–233.
4. Anderson, F.E. Phylogeny and historical biogeography of the loliginid squids (Mollusca: Cephalopoda) based on mitochondrial DNA sequence data. *Mol. Phylogenet. Evol.* **2000**, *15*, 191–214. [CrossRef]
5. Guo, J.; Zhang, C.; Li, Z.; Liu, D.; Tian, Y. Latitudinal Difference in the Condition Factor of Two Loliginidae Squid (Beka Squid and Indian Squid) in China Seas. *Diversity* **2023**, *15*, 812. [CrossRef]
6. Pang, Y.; Tian, Y.; Fu, C.; Wang, B.; Li, J.; Ren, Y.; Wan, R. Variability of coastal cephalopods in overexploited China Seas under climate change with implications on fisheries management. *Fish. Res.* **2018**, *208*, 22–33. [CrossRef]
7. David, G.K.; Marshall, D.J.; Riginos, C. Latitudinal variability in spatial genetic structure in the invasive ascidian, *Styela plicata*. *Mar. Biol.* **2010**, *157*, 1955–1965. [CrossRef]
8. Lopez-Barrera, G.; Ochoa-Zavala, M.; Quesada, M.; Harvey, N.; Nunez-Farfan, J.; Gonzalez-Rodriguez, A.; Rocha-Ramirez, V.; Oyama, K. Genetic imprints of *Brosimum alicastrum* Sw. in Mexico. *Am. J. Bot.* **2021**, *108*, 1793–1807. [CrossRef]
9. Zhao, L.; Wang, S.; Qu, F.; Liu, Z.; Gao, T. A genetic assessment of the population structure and demographic history of *Odontamblyopus lacepedii* (Perciformes, Amblyopinae) from the northwestern Pacific. *ZooKeys* **2022**, *1088*, 1–15. [CrossRef]
10. Williams, R.C.; Jackson, B.C.; Duvaux, L.; Dawson, D.A.; Burke, T.; Sinclair, W. The genetic structure of *Nautilus pompilius* populations surrounding Australia and the Philippines. *Mol. Ecol.* **2015**, *24*, 3316–3328. [CrossRef]
11. Zheng, X.; Lv, Y.; Lu, C. Species Diversity of Cephalopods in the China Seas. *Period. Ocean Univ. China* **2023**, *53*, 1–18.
12. Peter, R.J.; Chembian, A.J. Length-weight relationship and morphometric studies of the little squid *Loliolus* (*Nipponololigo*) *uyii* (Wakiya & Ishikawa, 1921) from the east coast, Tamil Nadu. *J. Exp. Zool. India* **2022**, *25*, 875–882.
13. Xu, R.; Lü, Y.; Tang, Y.; Chen, Z.; Xu, C.; Zhang, X.; Zheng, X. DNA Barcoding Reveals High Hidden Species Diversity of Chinese Waters in the Cephalopoda. *Front. Mar. Sci.* **2022**, *9*, 830381. [CrossRef]
14. Sheerin, E.; Barnwall, L.; Abad, E.; Larivain, A.; Oesterwind, D.; Petroni, M.; Perales-Raya, C.; Robin, J.; Sobrino, I.; Valeiras, J.; et al. Multi-method approach shows stock structure in *Loligo forbesii* squid. *ICES J. Mar. Sci.* **2022**, *79*, 1159–1174. [CrossRef]
15. Ching, T.; Chen, C.; Yagishita, N.; Yamaguchi, A.; Wang, C.; Shen, K. Variations in life-history traits and statolith shape for *Sepioteuthis* spp. in the waters off southwestern Japan. *Fish. Sci.* **2021**, *87*, 173–185. [CrossRef]
16. Vaseeharan, B.; Rajakamaran, P.; Jayaseelan, D.; Vincent, A.Y. Molecular markers and their application in genetic diversity of penaeid shrimp. *Aquacult. Int.* **2013**, *21*, 219–241. [CrossRef]
17. Strugnell, J.; Norman, M.; Jackson, J.; Drummond, A.J.; Cooper, A. Molecular phylogeny of coleoid cephalopods (Mollusca: Cephalopoda) using a multigene approach; the effect of data partitioning on resolving phylogenies in a Bayesian framework. *Mol. Phylogenet. Evol.* **2005**, *37*, 426–441. [CrossRef]
18. Sanchez, G.; Setiamarga, D.H.E.; Tuanapaya, S.; Tongtherm, K.; Winkelmann, I.E.; Schmidbaur, H.; Umino, T.; Albertin, C.; Allcock, L.; Perales-Raya, C.; et al. Genus-level phylogeny of cephalopods using molecular markers: Current status and problematic areas. *PeerJ* **2018**, *6*, e4331. [CrossRef]
19. Raj, N.; Sukumaran, S.; Jose, A.; Nisha, K.; Roul, S.K.; Rahangdale, S.; Kizhakudan, S.J.; Gopalakrishnan, A. Population genetic structure of Randall's threadfin bream *Nemipterus randalli* in Indian waters based on mitochondrial and nuclear gene sequences. *Sci. Rep.* **2024**, *14*, 7556. [CrossRef]

20. Xu, R.; Bo, Q.; Zheng, X. A divergent lineage among *Octopus minor* (Sasaki, 1920) populations in the Northwest Pacific supported by DNA barcoding. *Mar. Biol. Res.* **2018**, *14*, 335–344. [CrossRef]
21. Guo, B.; Ye, Y.; Li, J.; Qi, P.; Lv, Z.; Guan, A.; Wu, C. Genetic diversity and population structure of *Sepiella japonica* (Mollusca: Cephalopoda: Decapoda) inferred by 16S rDNA variations. *Aquac. Res.* **2016**, *47*, 3016–3022. [CrossRef]
22. Li, S.; Lyu, Y.; Zhang, C.; Zheng, X. Morphological and Genetic Differentiation of *Loliolus* (*Nipponololigo*) *beka* (Cephalopoda: Loliginidae) in Coastal China. *Diversity* **2023**, *15*, 41. [CrossRef]
23. Zheng, J.; Tang, Y.; Xu, R.; Zhang, X.; Zheng, X. Molecular phylogenetics and population demographic history of *Amphioctopus fangsiao*, inferred from mitochondrial and microsatellite DNA markers. *Acta Oceanol. Sin.* **2023**, *42*, 39–48. [CrossRef]
24. Graybeal, A. Evaluating the phylogenetic utility of genes: A search for genes informative about deep divergences among vertebrates. *Syst. Biol.* **1994**, *43*, 174–193. [CrossRef]
25. Muhammad, F.; Lu, Z.; Liu, L.; Gong, L.; Du, X.; Shafi, M.; Kaleri, H.A. Genetic structure of *Octopus minor* around Chinese waters as indicated by nuclear DNA variations (Mollusca, Cephalopoda). *ZooKeys* **2018**, *775*, 1–14. [CrossRef] [PubMed]
26. Villanueva, R.; Arkhipkin, A.; Jereb, P.; Lefkaditou, E.; Lipinski, M.R.; Perales-Raya, C.; Riba, J.; Rocha, F. Embryonic life of the loliginid squid *Loligo vulgaris*: Comparison between statoliths of Atlantic and Mediterranean populations. *Mar. Ecol. Prog. Ser.* **2003**, *253*, 197–208. [CrossRef]
27. Arkhipkin, A.I. Statoliths as 'black boxes' (life recorders) in squid. *Mar. Freshw. Res.* **2005**, *56*, 573–583. [CrossRef]
28. Green, C.P.; Robertson, S.G.; Hamer, P.A.; Virtue, P.; Jackson, G.D.; Moltschaniwskyj, N.A. Combining statolith element composition and Fourier shape data allows discrimination of spatial and temporal stock structure of arrow squid (*Nototodarus gouldi*). *Can. J. Fish. Aquat. Sci.* **2015**, *72*, 1609–1618. [CrossRef]
29. Chen, X.J.; Liu, B.L.; Fang, Z.; Li, J.H. *Cephalopoda*; China Ocean Press: Beijing, China, 2019; pp. 68–69.
30. Winnepenninckx, B.; Backeljau, T.; De Wachter, R. Extraction of high molecular weight DNA from molluscs. *Trends Genet.* **1993**, *9*, 407.
31. Folmer, O.; Black, M.; Hoeh, W.; Lutz, R.; Vrijenhoek, R. DNA primers for amplification of mitochondrial cytochrome c oxidase subunit I from diverse metazoan invertebrates. *Mol. Mar. Biol. Biotechnol.* **1994**, *3*, 294–299.
32. Palumbi, S.; Martin, A.; Romano, S.; McMillan, W.O.; Stice, L.; Grabowski, G. *The Simple Fool's Guide to PCR*; Department of Zoology Special Publication, University of Hawaii: Honolulu, HI, USA, 1991.
33. Swindell, S.R.; Plasterer, T.N. Seqman. In *Sequence Data Analysis Guidebook*; Springer: Totowa, NJ, USA, 1997; pp. 75–89.
34. Tamura, K.; Stecher, G.; Kumar, S. MEGA11: Molecular Evolutionary Genetics Analysis Version 11. *Mol. Biol. Evol.* **2021**, *38*, 3022–3027. [CrossRef] [PubMed]
35. Rozas, J.; Ferrer-Mata, A.; Sanchez-DelBarrio, J.C.; Guirao-Rico, S.; Librado, P.; Ramos-Onsins, S.E.; Sanchez-Gracia, A. DnaSP 6: DNA Sequence Polymorphism Analysis of Large Data Sets. *Mol. Biol. Evol.* **2017**, *34*, 3299–3302. [CrossRef] [PubMed]
36. Leigh, J.W.; Bryant, D. POPART: Full-feature software for haplotype network construction. *Methods Ecol. Evol.* **2015**, *6*, 1110–1116. [CrossRef]
37. Tajima, F. Statistical method for testing the neutral mutation hypothesis by DNA polymorphism. *Genetics* **1989**, *123*, 585–595. [CrossRef] [PubMed]
38. Fu, Y.X. Statistical tests of neutrality of mutations against population growth, hitchhiking and background selection. *Genetics* **1997**, *147*, 915–925. [CrossRef]
39. Excoffier, L.; Lischer, H.E. Arlequin suite ver 3.5: A new series of programs to perform population genetics analyses under Linux and Windows. *Mol. Ecol. Resour.* **2010**, *10*, 564–567. [CrossRef]
40. Zhang, D.; Gao, F.; Jakovlic, I.; Zou, H.; Zhang, J.; Li, W.X.; Wang, G.T. PhyloSuite: An integrated and scalable desktop platform for streamlined molecular sequence data management and evolutionary phylogenetics studies. *Mol. Ecol. Resour.* **2020**, *20*, 348–355. [CrossRef]
41. Kalyaanamoorthy, S.; Minh, B.Q.; Wong, T.; Von Haeseler, A.; Jermiin, L.S. ModelFinder: Fast model selection for accurate phylogenetic estimates. *Nat. Methods* **2017**, *14*, 587–589. [CrossRef]
42. Nguyen, L.T.; Schmidt, H.A.; von Haeseler, A.; Minh, B.Q. IQ-TREE: A fast and effective stochastic algorithm for estimating maximum-likelihood phylogenies. *Mol. Biol. Evol.* **2015**, *32*, 268–274. [CrossRef]
43. Ronquist, F.; Teslenko, M.; van der Mark, P.; Ayres, D.L.; Darling, A.; Hohna, S.; Larget, B.; Liu, L.; Suchard, M.A.; Huelsenbeck, J.P. MrBayes 3.2: Efficient Bayesian phylogenetic inference and model choice across a large model space. *Syst. Biol.* **2012**, *61*, 539–542. [CrossRef]
44. Natsukari, Y.; Nakanose, T.; Oda, K. Age and growth of loliginid squid *Photololigo edulis* (Hoyle, 1885). *J. Exp. Mar. Biol. Ecol.* **1988**, *116*, 177–190. [CrossRef]
45. Moustahfid, H. Age and growth of arrow squid *Todarodes sagittatus* (Cephalopoda: Ommastrephidae) sampled in summer in Atlantic Moroccan waters. *Bull. Mar. Sci.* **2002**, *71*, 535–543.
46. Libungan, L.A.; Palsson, S. ShapeR: An R Package to Study Otolith Shape Variation among Fish Populations. *PLoS ONE* **2015**, *10*, e0121102. [CrossRef] [PubMed]
47. Breiman, L. Random Forests. *Mach. Learn.* **2001**, *45*, 5–32. [CrossRef]
48. Wei, D.; Zheng, S.; Wang, S.; Yan, J.; Liu, Z.; Zhou, L.; Wu, B.; Sun, X. Genetic and Haplotype Diversity of Manila Clam *Ruditapes philippinarum* in Different Regions of China Based on Three Molecular Markers. *Animals* **2023**, *13*, 2886. [CrossRef]

49. Bazin, E.; Glemin, S.; Galtier, N. Population size does not influence mitochondrial genetic diversity in animals. *Science* **2006**, *312*, 570–572. [CrossRef]
50. Wu, T.; Sun, C.; Lao, Y.; Zhang, Q. Genetic diversity and population structure of threeline grunt *Parapristipoma trilineatum* (Perciformes: Haemulidae) in China and Japan based on mtDNA control region. *Glob. Ecol. Conserv.* **2024**, *53*, e03038. [CrossRef]
51. Tajima, F. Evolutionary relationship of DNA sequences in finite populations. *Genetics* **1983**, *105*, 437–460. [CrossRef]
52. Grant, W.A.S.; Bowen, B.W. Shallow population histories in deep evolutionary lineages of marine fishes: Insights from sardines and anchovies and lessons for conservation. *J. Hered.* **1998**, *89*, 415–426. [CrossRef]
53. Rand, D.M. Thermal habit, metabolic rate and the evolution of mitochondrial DNA. *Trends Ecol. Evol.* **1994**, *9*, 125–131. [CrossRef]
54. Gong, J. Genetic Diversity of Penis Fish (*Urechis unicinctus*) Based on Mitochondrial and Nuclear Gene Sequences. Master's Thesis, Ludong University, Yantai, China, 2018.
55. Avise, J.C. *Molecular Markers, Natural History and Evolution*, 2nd ed.; Sinauer Associates: Sunderland, MA, USA, 2004; p. 47.
56. Palumbi, S.R. Genetic-divergence, reproductive isolation, and marine speciation. *Annu. Rev. Ecol. Syst.* **1994**, *25*, 547–572. [CrossRef]
57. Lopez-Marquez, V.; Cushman, S.A.; Templado, J.; Wan, H.Y.; Bothwell, H.M.; Machordom, A. Genetic connectivity of two marine gastropods in the Mediterranean Sea: Seascape genetics reveals species-specific oceanographic drivers of gene flow. *Mol. Ecol.* **2021**, *30*, 4608–4629. [CrossRef] [PubMed]
58. Li, X.; Ma, J.; Liu, Y.; Hu, S.; Sun, W.; Nan, F.; Shen, C. A monthly resolved coral δ13C and δ18O record of changes in the Kuroshio Current into the South China Sea via the Luzon Strait. *Palaeogeogr. Palaeocl.* **2023**, *615*, 111468. [CrossRef]
59. Hu, J.; Kawamura, H.; Hong, H.; Qi, Y. A Review on the Currents in the South China Sea: Seasonal Circulation, South China Sea Warm Current and Kuroshio Intrusion. *J. Oceanogr.* **2000**, *56*, 607–624. [CrossRef]
60. Lin, T.; Liu, L. Low Levels of Genetic Differentiation among Populations of the Coral-Inhabiting Snail *Coralliophila violacea* (Gastropoda: Coralliophilidae) in Regions of the Kuroshio and South China Sea. *Zool. Stud.* **2008**, *47*, 17–24.
61. Zhu, J.; Hu, J.; Zheng, Q. An overview on water masses in the China seas. *Front. Mar. Sci.* **2022**, *9*, 972921. [CrossRef]
62. Juarez, O.E.; Arreola-Meraz, L.; Sanchez-Castrejon, E.; Avila-Poveda, O.H.; Lopez-Galindo, L.L.; Rosas, C.; Galindo-Sanchez, C.E. Oviducal gland transcriptomics of *Octopus maya* through physiological stages and the negative effects of temperature on fertilization. *PeerJ* **2022**, *10*, e12895. [CrossRef]
63. Dominguez-Estrada, A.; Galindo-Sanchez, C.E.; Ventura-Lopez, C.; Rosas, C.; Juarez, O.E. Response of optic gland pathways to thermal stress in the reproductive phase of female *Octopus maya*. *J. Mollus. Stud.* **2022**, *88*, eyac018. [CrossRef]
64. Juárez, O.E.; Galindo-Sánchez, C.E.; Díaz, F.; Re, D.; Sánchez-García, A.M.; Camaal-Monsreal, C.; Rosas, C. Is temperature conditioning *Octopus maya* fitness? *J. Exp. Mar. Biol. Ecol.* **2015**, *467*, 71–76. [CrossRef]
65. Hewitt, G. The genetic legacy of the Quaternary ice ages. *Nature* **2000**, *405*, 907–913. [CrossRef]
66. Wang, P. Response of Western Pacific marginal seas to glacial cycles: Paleoceanographic and sedimentological features. *Mar. Geol.* **1999**, *156*, 5–39. [CrossRef]
67. Shen, K.N.; Jamandre, B.W.; Hsu, C.C.; Tzeng, W.N.; Durand, J.D. Plio-Pleistocene sea level and temperature fluctuations in the northwestern Pacific promoted speciation in the globally-distributed flathead mullet *Mugil cephalus*. *BMC Evol. Biol.* **2011**, *11*, 83. [CrossRef] [PubMed]
68. Zhao, D.; Li, Q.; Kong, L.; Yu, H. Cryptic diversity of marine gastropod *Monodonta labio* (Trochidae), did the early Pleistocene glacial isolation and sea surface temperature gradient jointly drive diversification of sister species and/or subspecies in the Northwestern Pacific? *Mar. Ecol.* **2017**, *38*, e12443. [CrossRef]
69. Dommergues, J.L.; Neige, P.; Von Boletzky, S. Exploration of morphospace using Procrustes analysis in statoliths of cuttlefish and squid (Cephalopoda: Decabrachia)-Evolutionary aspects of form disparity. *Veliger Berkeley* **2000**, *43*, 265–276.
70. Ching, T.; Yagishita, N.; Yamaguchi, A.; Wang, C.; Chen, C. Geographical variations in genetic group composition, life-history traits, and statolith shape for *Sepioteuthis* spp. in the Northwest Pacific. *Mar. Freshw. Res.* **2022**, *73*, 995–1010. [CrossRef]
71. Guo, J.Z.; Liu, D.; Zhang, C.; Tian, Y.J.; Li, Z.X. Using statolith shape analysis to identify five commercial Loliginidae squid species in Chinese waters. *J. Oceanol. Limnol.* **2021**, *39*, 1160–1167. [CrossRef]
72. Bobowski, B.T.C.; Power, A.M.; Burns, F.; Carbonara, P.; Cuccu, D.; Donnaloia, M.; Follesa, M.C.; Moreno, A.; Sokolova, I.M.; Valls, M.; et al. Stock discrimination of two European squids (*Illex coindetii*, *Loligo forbesii*) by statolith shape analysis. *Fish. Manag. Ecol.* **2024**, *31*, e12689. [CrossRef]
73. Vignon, M.; Morat, F. Environmental and genetic determinant of otolith shape revealed by a non-indigenous tropical fish. *Mar. Ecol. Prog. Ser.* **2010**, *411*, 231–241. [CrossRef]

Disclaimer/Publisher's Note: The statements, opinions and data contained in all publications are solely those of the individual author(s) and contributor(s) and not of MDPI and/or the editor(s). MDPI and/or the editor(s) disclaim responsibility for any injury to people or property resulting from any ideas, methods, instructions or products referred to in the content.